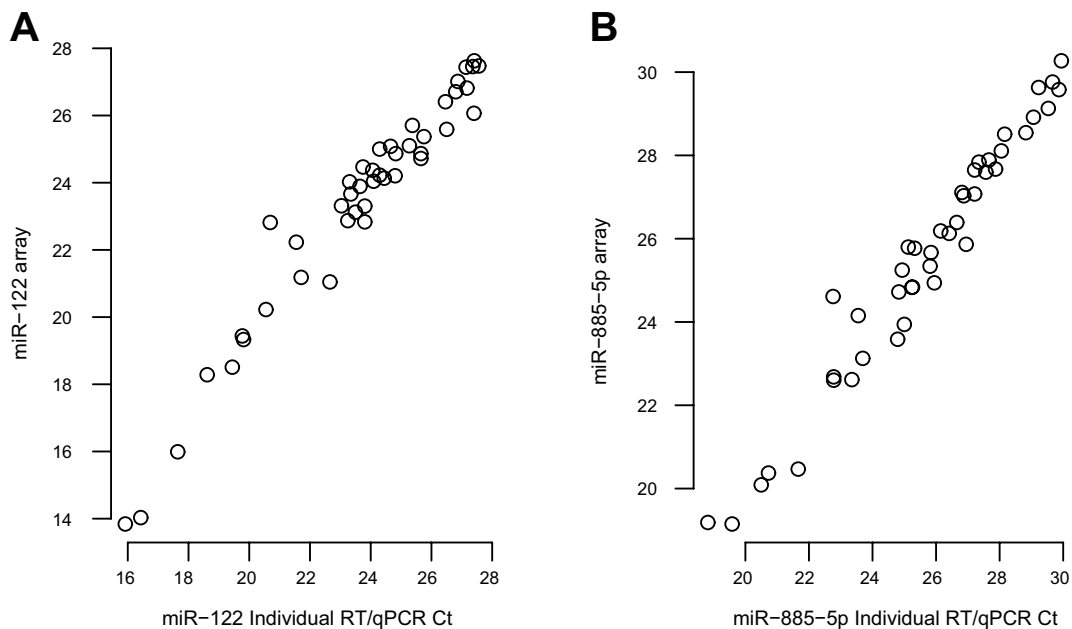


1
2 **Supplementary Figure 1. Quantitative PCR array performance characteristics**
3 **indicate that miRNA quantification and detection was unbiased. (A)** The number of
4 microRNAs detected per sample and **(B)** the median qPCR crossing threshold (Ct)
5 values among all measured miRNAs per sample are shown across all time points. **(C)**
6 Median Ct values of the externally added control miRNA ath-miR-159a for all samples.
7 Ath-miR-159a was separately included on each array > 10 times to improve the
8 precision of its measurement. **(D)** miRNAs were ordered by their detection frequency
9 (100*the number of samples in which a miRNA was detected divided by the total
10 number of samples) in all samples from participants in the discovery cohort who
11 developed acute HCV infection: 243 miRNAs were detected in > 70% of samples, and
12 these were included in the final unbiased analysis.

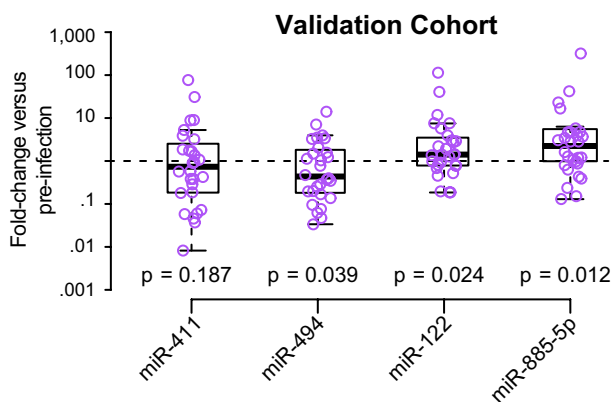
13



14

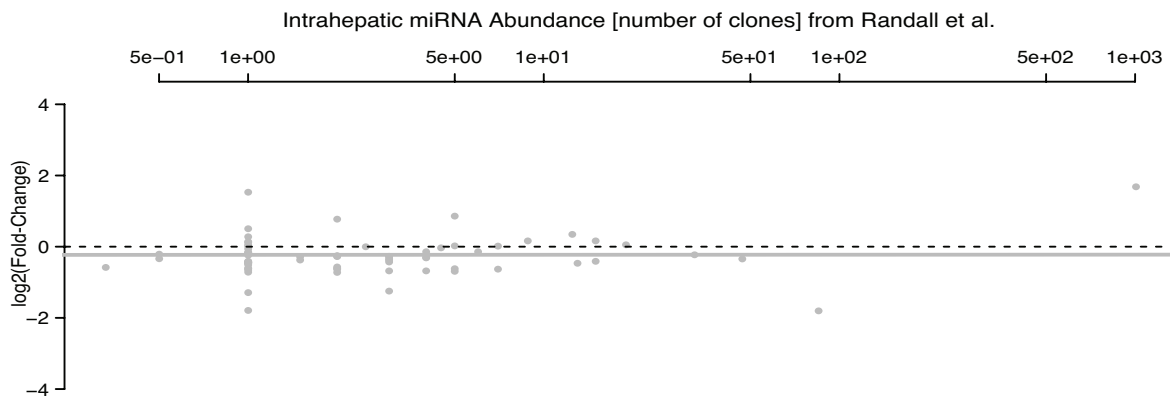
15 **Supplementary Figure 2. Validation of qPCR array results using individual**
16 **RT/qPCR assays for select miRNAs. (A)** miR-122 and **(B)** miR-885-5p abundance at
17 pre-infection and initial-viremia time points for all infected individuals in the discovery
18 cohort were confirmed using individual RT/qPCR Cts; qPCR array results compared
19 favorably with individual RT/qPCR results ($r>0.97$, $p<2.2 \times 10^{-16}$ for both).
20

21



22

23 **Supplementary Figure 3. Validation of the plasma miRNA signature of acute HCV**
24 **in a separate cohort.** Boxplots with individual values show the changes in circulating
25 miRNA abundance for miR-411, miR-494, miR-122, and miR-885-5p between pre-
26 viremia and initial viremia in 28 participants of the UFO study. P-values generated by
27 the non-parametric Wilcoxon rank-sum test are shown for the plotted miRNAs.
28

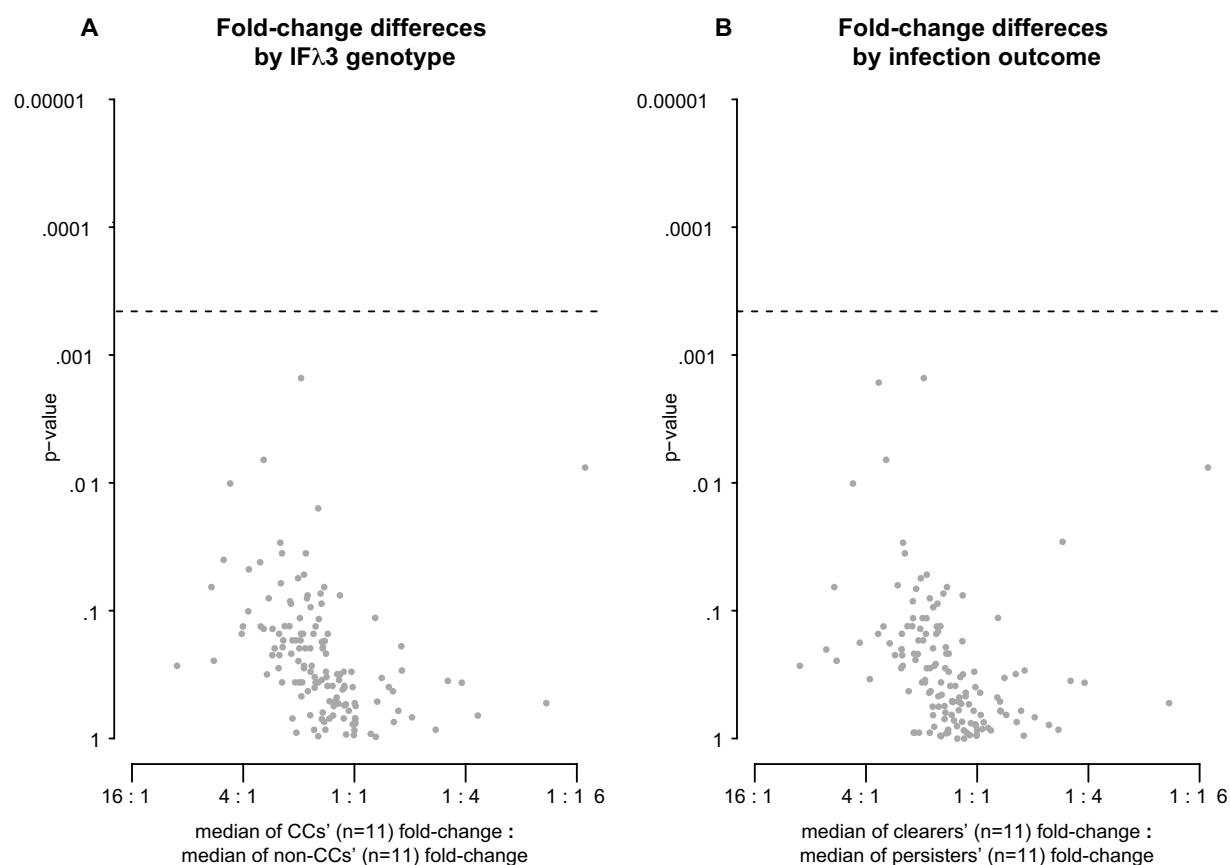


29

30 **Supplementary Figure 4. Plasma miRNA abundance is not related to intrahepatic**
31 **miRNA abundance.** The plasma miRNA abundance at initial viremia for each of 70
32 miRNAs (y-axes) was compared to the intrahepatic abundance of the same miRNAs (x-
33 axes), based on previously published data[1].

34 [1] Randall G, Panis M, Cooper JD, Tellinghuisen TL, Sukhodolets KE, Pfeffer S, et al.
35 Cellular cofactors affecting hepatitis C virus infection and replication. Proc Natl Acad
36 Sci U S A 2007;104:12884–9. doi:10.1073/pnas.0704894104.

37

38
39

40

41 **Supplementary Figure 5. Changes in miRNA abundance did not significantly**
 42 **differ by *IFNL3* genotype or infection outcome.** Fold-changes between pre-infection
 43 and initial viremia were separated into groups according to **(A) *IFNL3* genotype** or **(B)**
 44 **infection outcome** and each group was assigned a median fold change (n=11 for CC,
 45 nonCC [CT or TT], clearers, and persisters). The volcano plots depict the differences in
 46 the median fold-changes between each group in the x-axes in the form of a ratio (higher
 47 fold-change in the non-CTs or persisters to the left). In the y-axis is shown the
 48 uncorrected p-value of the change in miRNA abundance. The dashed lines indicate the
 49 threshold for significance.